Inner-Sphere Electron Transfer in Organic Chemistry. Relevance to Electrophilic Aromatic Nitration†

JAY K. KOCHI

Chemistry Department, University of Houston, Houston, Texas 77204-5641

Received August 21, 1991 (Revised Manuscript Received October 25, 1991)

Introduction

Physical organic chemistry centers around a multitude of reaction mechanisms for which the following insights have been wisely provided to us.[1]

ON THE DETERMINATION OF REACTION MECHANISMS

A reaction mechanism is a detailed description of a reacting system as it progresses from reactants to products. It includes identification of all intermediates that are involved, assessment of the characteristics of the transition state(s) through which the reaction progresses, and recognition of the factors that affect reactivity....

...one cannot expect to know or to prove a reaction mechanism in an absolute sense. The chemist can often reject conceivable mechanisms on the basis of experimental evidence and thereby narrow the field of possibilities, perhaps till only one remains....

...but how can one know whether there remains an inconceivable mechanism that is in full accord with the facts?

J. F. Bunnett

In the spirit of the invaluable lessons taught here, I wish to reconsider the conventional view of electrophilic aromatic substitution, since it forms a critical cornerstone of reaction mechanisms[2] as enunciated in contemporary elementary textbooks for organic chemistry. Among the various substitution processes, it is particularly noteworthy that aromatic nitration has elicited wide interest stemming from the early and unambiguous identification of the nitronium ion (NO_2^+) as the active electrophile from nitric acid.[3] As broadly conceived, the seminal mechanistic question focuses on the activation process(es) leading up to the Wheland or σ-intermediate,[4] generally considered to involve the *direct* addition of the electrophilic NO_2^+ to the aromatic substrate, viz.,[5]

$$NO_2^+ + ArH \longrightarrow Ar\overset{+}{\underset{NO_2}{H}} \text{ etc.} \qquad (1)$$

However, there is an alternative, *stepwise* mechanism which identifies NO_2^+ as an oxidant in a rate-limiting electron transfer, i.e.,[6]

$$NO_2^+ + ArH \longrightarrow \underset{\mathbf{I}}{[NO_2, ArH^+\cdot]} \xrightarrow{\text{fast}} Ar\overset{+}{\underset{NO_2}{H}} \qquad (2)$$

Since such a mechanistic ambiguity between the heterolytic (2-electron) and homolytic (1-electron) pathways is inherent to many organic reactions, it is important for us to establish in this Account the experimental basis for the distinctive intermediate such as I in eq 2. Thus the properties and behavior of the ion radical pair are crucial to establishing its relationship with the numerous facets[7] of electrophilic aromatic nitration. For these reasons, it is especially important to know whether pair I will actually lead to the Wheland intermediate, and in the amounts necessary to establish the isomer distributions commonly observed in aromatic nitrations.[8] However, the independent proof of this type of ion radical pair has not been forthcoming owing to its expectedly transitory existence, the annihilation of I being perforce faster than the rate (constant) for production. Since the latter is a kinetics restriction placed only on thermal transformations, let us consider how the ion radical pair can be spontaneously produced by the vertical (nonadiabatic) activation of charge-transfer complexes and its reactivity directly measured by time-resolved spectroscopy.

Formation and Activation of Aromatic EDA Complexes with Nitrating Agents

The electrophilic NO_2^+ and nitronium "carriers" NO_2Y such as nitric acid, acetyl nitrate, dinitrogen pentoxide, nitryl chloride, *N*-nitropyridinium, tetranitromethane, etc. with Y = OH^-, OAc^-, NO_3^-, Cl^-, Py, and $C(NO_2)_3^-$, respectively, are all electron deficient and thus capable of serving as effective electron acceptors in common with other nitro compounds.[9] A charac-

Jay K. Kochi was born in Los Angeles and educated at Cornell University and UCLA. He obtained his Ph.D. degree at Iowa State University with George Hammond in 1952. After an instructorship at Harvard University (Louis Fieser) and NIH Special Fellowship at Cambridge University (Lord Alexander Todd), he was at Shell Development Co. in Emeryville, CA, until 1962. He reentered academic work at Case Institute of Technology and moved to Indiana University in 1969 and then to the University of Houston in 1984.

† Dedicated to Professor J. F. Bunnett on the occasion of his retirement.

(1) Bunnett, J. F. In *Investigation of Rates and Mechanisms of Reactions, Part I*; Bernasconi, C. F., Ed.; Wiley: New York, 1986; pp 253, 361.

(2) Ingold, C. K. *Structure and Mechanism in Organic Chemistry*, 2nd ed.; Cornell Press: Ithaca, NY, 1969. See also: Taylor, R. *Electrophilic Aromatic Substitution*; Wiley: New York, 1990.

(3) Olah, G. A.; Malhotra, R.; Narang, S. C. *Nitration*; VCH: New York, 1989.

(4) Wheland, G. W. *J. Am. Chem. Soc.* **1942**, *64*, 900. See also: Guk, Yu. V.; Ilyushin, M. A.; Golod, E. L.; Gidaspov, B. V. *Russ. Chem. Rev.* **1983**, *52*, 284.

(5) Schofield, K. *Aromatic Nitration*; Cambridge Press: New York, 1980.

(6) Nagakura, S.; Tanaka, J. *J. Chem. Phys.* **1954**, *22*, 563. Brown, R. D. *J. Chem. Soc.* **1959**, 2224, 2232. Perrin, C. L. *J. Am. Chem. Soc.* **1977**, *99*, 5516. See also: Schmitt, R. J.; Buttrill, S. E., Jr.; Ross, D. S. *J. Am. Chem. Soc.* **1984**, *106*, 926 (gas phase).

(7) Hartshorn, S. R. *Chem. Soc. Rev.* **1974**, *3*, 167. Suzuki, H. *Synthesis* **1977**, 217.

(8) Stock, L. M.; Brown, H. C. *Adv. Phys. Org. Chem.* **1963**, *1*, 35.

(9) Feuer, H., Ed. *Chemistry of the Nitro and Nitroso Groups*; Wiley: New York, 1969. Chowdhury, S.; Kishi, H.; Dillow, G. W.; Kebarle, P. *Can. J. Chem.* **1989**, *67*, 603.

0001-4842/92/0125-0039$03.00/0

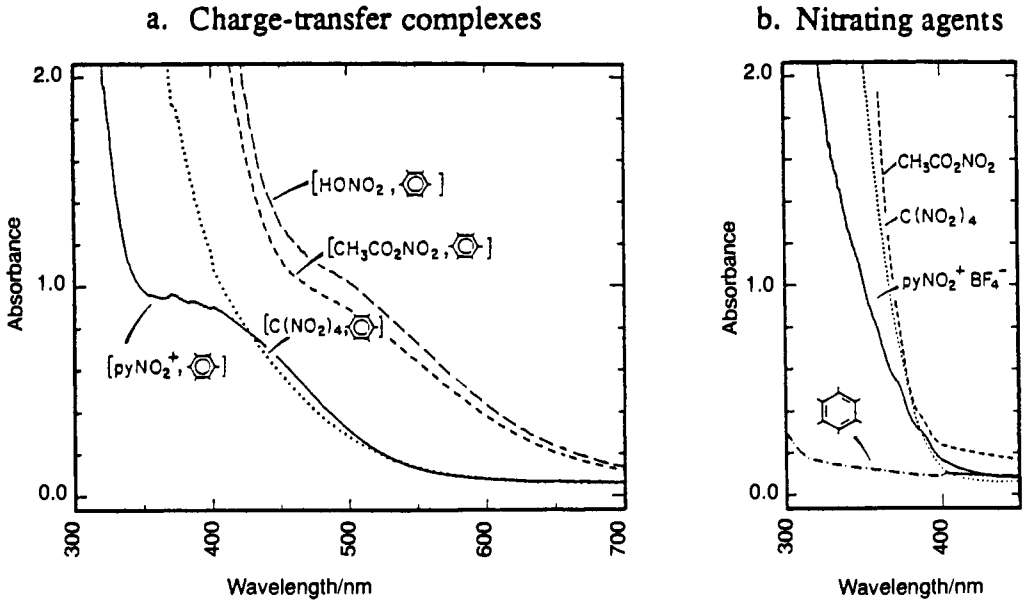

Figure 1. (a) Comparative charge-transfer spectra of aromatic EDA complexes with various nitrating agents (as indicated) relative to (b) the absorption spectra of the uncomplexed donor (hexamethylbenzene) and acceptors.[27]

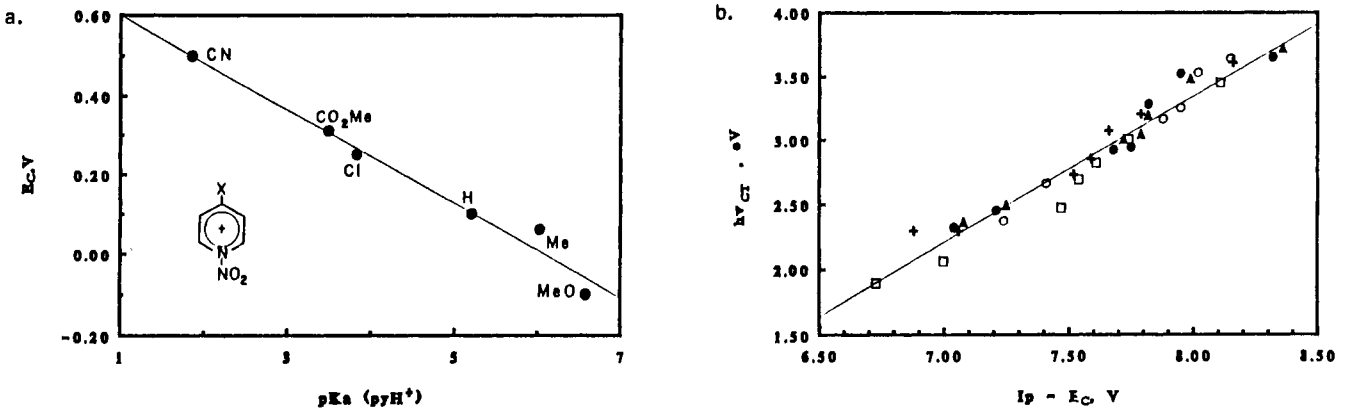

Figure 2. Variation of (a) the acceptor strength (E_c) of X–$PyNO_2^+$ with the thermodynamic stability (pK_a) of X–PyH^+ and (b) the CT transition energy ($h\nu_{CT}$) with the (HOMO–LUMO) gap between ArH donors and X–$PyNO_2^+$ acceptors in various EDA complexes.[15]

teristic property of the latter is their ability to form electron donor–acceptor or EDA complexes with different types of electron-rich donors, including aromatic hydrocarbons, i.e.,[10]

$$NO_2Y + ArH \underset{}{\overset{K_{EDA}}{\rightleftharpoons}} [NO_2Y,ArH] \qquad (3)$$

Such EDA complexes are frequently referred to as charge-transfer (CT) complexes,[11] since they are often colored and exhibit intermolecular absorption bands ($h\nu_{CT}$) that have been spectroscopically characterized by Mulliken.[12] Indeed the common family of charge-transfer spectra in Figure 1 establishes the various nitrating agents to be uniformly engaged as electron acceptors in aromatic EDA complexes. The systematic and quantitative study of structural effects of the nitrating agent is possible with related *N*-nitropyridinium cations[13] (para-substituted with X = CH_3O, CH_3, H, Cl, CO_2CH_3, and CN groups) to represent a graded series of increasingly powerful electron acceptors (see Figure 2a). Coupled with different arenes, each X–$PyNO_2^+$ acceptor forms EDA complexes that consistently show the characteristic red shift[11] of the charge-transfer band with increasing donor strengths in the order[14] mesitylene < durene < pentamethylbenzene < dimethylnaphthalene < methylanthracene. The global effect of all these ArH/X–$PyNO_2^+$ combinations on the charge-transfer energies of the EDA complexes (Figure 2b) is encompassed within a single Mulliken correlation which spans the HOMO–LUMO gap of almost 50 kcal mol^{-1}, i.e.,

$$h\nu_{CT} = IP - E_c - 5 \qquad (4)$$

where IP is the ionization potential of the aromatic donor, E_c is a reduction potential of the X–$PyNO_2^+$ acceptor, and both are expressed in volts.[14,15] The aromatic EDA complexes with different nitrating agents [ArH,NO_2Y] are also classified as weak, and they are

(10) Andrews, L. J.; Keefer, R. M. *Molecular Complexes in Organic Chemistry*; Holden-Day: San Francisco, 1964. Briegleb, G. *Elektronen-Donator Komplexe*; Springer: Berlin, 1961. Hanna, M. W.; Lippert, J. L. In *Molecular Complexes*; Foster, R., Ed.; Elek: London, 1973; p 2 ff.

(11) Foster, R. *Organic Charge-Transfer Complexes*; Academic: New York, 1969.

(12) Mulliken, R. S. *J. Am. Chem. Soc.* **1952**, *74*, 811. Mulliken, R. S.; Person, W. B. *Molecular Complexes*; Wiley: New York, 1969.

(13) Olah, G. A.; Narang, S. C.; Olah, J. A.; Pearson, R. L.; Cupas, C. A. *J. Am. Chem. Soc.* **1980**, *102*, 3507.

(14) Howell, J. O.; Goncalves, J. M.; Amatore, C.; Klasinc, L.; Wightman, R. M.; Kochi, J. K. *J. Am. Chem. Soc.* **1984**, *106*, 3968. Masnovi, J. M.; Seddon, E. A.; Kochi, J. K. *Can. J. Chem.* **1984**, *62*, 2552.

(15) Kim, E. K.; Lee, K. Y.; Kochi, J. K. *J. Am. Chem. Soc.*, in press.

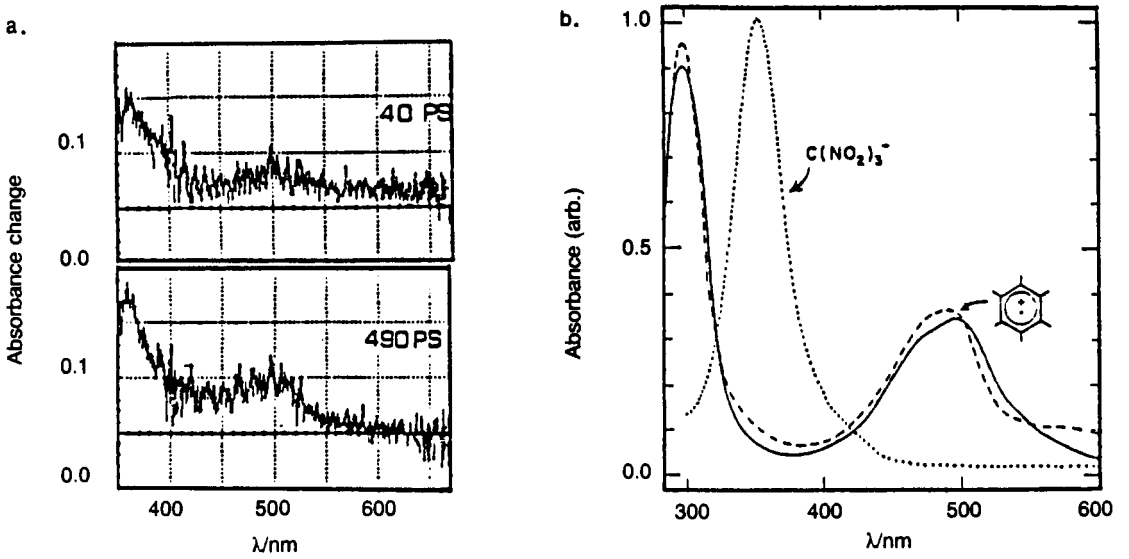

Figure 3. (a) Time-resolved absorption spectra at 40 and 490 ps following the 532-nm laser pulse excitation of the hexamethylbenzene EDA complex with tetranitromethane. (b) Absorption spectra of $HMB^{+\bullet}$ generated spectroelectrochemically and $C(NO_2)_3^-$ obtained from the salt. Reprinted with permission from ref 20. Copyright 1986 American Chemical Society.

present in low steady-state concentrations owing to the limited magnitudes of their formation constants K_{EDA} (eq 3), as measured by the Benesi–Hildebrand spectrophotometric method.[16]

Activation of the various [NO_2Y,ArH] complexes can be thermally or photochemically programmed to effect aromatic nitration. For example, the bright lemon color immediately attendant upon the mixing of $PyNO_2^+$ and naphthalene in acetonitrile slowly fades within an hour to afford a mixture of 1- and 2-nitronaphthalene in excellent yields.[17] The same isomeric mixture is obtained when the yellow solution is initially cooled down to −40 °C (to inhibit the thermal nitration), and then deliberately irradiated at $\lambda > 425$ nm with the lamp output passed through a sharp cutoff filter, i.e.,

$$PyNO_2^+ + ArH \xrightarrow[h\nu\ (-40\ ^\circ C)]{\Delta\ (25\ ^\circ C)\ or} ArNO_2 + PyH^+ \quad (5)$$

Inspection of the absorption spectrum of the yellow [$PyNO_2^+$,naphthalene] complex[18] similar to those shown in Figure 1 verifies the selective excitation of only the charge-transfer band at $\lambda_{CT} = 410$ nm by this filtered radiation. Thus there can be no ambiguity arising from the adventitious local excitation[12] of the uncomplexed reactants under these conditions, and the photochemical transformation in eq 5 is designated hereafter as *charge-transfer* ($h\nu_{CT}$) *nitration.*

Mechanism of Charge-Transfer Nitration: Time-Resolved Spectroscopy

Picosecond time-resolved spectroscopy has defined the relevant photophysical and photochemical processes associated with the charge-transfer excitation ($h\nu_{CT}$) of aromatic EDA complexes.[19] As applied to the nitrating acceptors NO_2Y, the formation of the pertinent ion radical pair I by charge-transfer excitation is summarized as follows:[20]

Scheme I

$$ArH + NO_2Y \overset{K_{EDA}}{\rightleftharpoons} [ArH,NO_2Y] \quad (6)$$

$$[ArH,NO_2Y] \overset{h\nu_{CT}}{\rightleftharpoons} [ArH^{+\bullet},NO_2Y^{\bullet-}] \quad (7)$$

$$[ArH^{+\bullet},NO_2Y^{\bullet-}] \xrightarrow{fast} \underset{I}{[ArH^{+\bullet},NO_2]Y^-} \quad (8)$$

Activation of the EDA complex by the specific irradiation of the CT absorption band results in the photoinduced electron transfer (eq 7) in accord with Mulliken theory;[12] and Figure 3 illustrates the subsequent fragmentation (eq 8) to afford the ion radical pair I from tetranitromethane (TNM) as the prototypical acceptor (compare Figure 1). The high quantum yields for charge-transfer nitration ($\Phi \sim 0.5$) relate directly to the efficiency of the irreversible fragmentation in eq 8 relative to energy wastage by back electron transfer in eq 7. Moreover, the short lifetime of $TNM^{\bullet-}$ ($\tau < 3$ ps)[21] ensures that $ArH^{+\bullet}$ and NO_2 are born as the ion radical pair I, initially trapped within the solvent cage, since this time scale obviates any competition from diffusional separation.

The excellent material balance obtained in the charge-transfer nitration of various aromatic substrates with TNM demands that the ion radical pair I in Scheme I proceeds quantitatively to the nitration products according to the stoichiometry in eq 9 when Y^- = trinitromethide.[22] Such a transformation must

$$\underset{I}{[ArH^{+\bullet},NO_2]Y^-} \rightarrow ArNO_2 + HY \quad (9)$$

(16) Benesi, H. G.; Hildebrand, J. H. *J. Am. Chem. Soc.* **1949**, *71*, 2703.
(17) Sankararaman, S.; Kochi, J. K. *J. Chem. Soc., Perkin Trans. 2* **1991**, 1.
(18) Figure 1 in ref 17.
(19) See: Nagakura, S. *Excited States*; Lin, E. C., Ed.; Academic: New York, 1975; Vol. 2, p 321 ff. Masuhara, H.; Mataga, N. *Acc. Chem. Res.* **1981**, *14*, 312. Goodman, J. L.; Peters, K. S. *J. Am. Chem. Soc.* **1985**, *107*, 6459. Gould, I. R.; Young, R. H.; Moody, R. E.; Farid, S. *J. Phys. Chem.* **1991**, *95*, 2068. Wallis, J. M.; Kochi, J. K. *J. Am. Chem. Soc.* **1988**, *110*, 8207 for leading references. For a review: Jones, G., II. In *Photoinduced Electron Transfer*; Fox, M. A., Chanon, M., Eds.; Elsevier: New York, 1988; Part A.
(20) Masnovi, J. M.; Hilinski, E. F.; Rentzepis, P. M.; Kochi, J. K. *J. Am. Chem. Soc.* **1986**, *108*, 1126.
(21) Rabani, J.; Mulac, W. A.; Matheson, M. S. *J. Phys. Chem.* **1965**, *69*, 53. Masnovi et al., ref 20.
(22) (a) Sankararaman, S.; Haney, W. A.; Kochi, J. K. *J. Am. Chem. Soc.* **1987**, *109*, 5235. (b) Sankararaman, S.; Haney, W. A.; Kochi, J. K. *J. Am. Chem. Soc.* **1987**, *109*, 7824. (c) Masnovi, J. M.; Kochi, J. K. *J. Org. Chem.* **1985**, *50*, 5245.

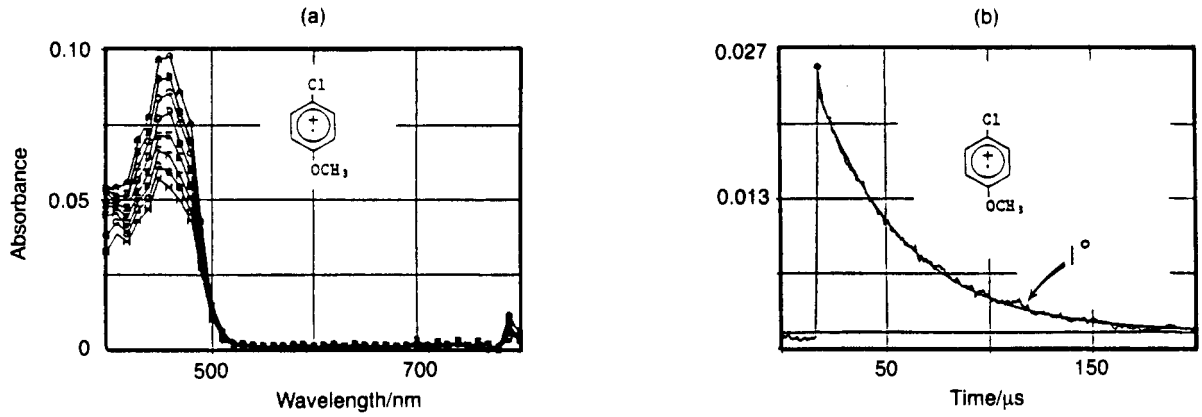

Figure 4. (a) Time-resolved absorption spectrum of the aromatic cation radical following the CT excitation of the tetranitromethane complex with arene (*p*-chloroanisole). (b) The fit of the experimental decay of $ArH^{\bullet+}$ to the Wheland intermediate by first-order kinetics is shown by the (superimposed) smooth curve obtained from the computer-generated least-squares treatment. Reprinted with permission from ref 22b. Copyright 1987 American Chemical Society.

Scheme II

$$[ArH^{+\cdot}, NO_2]\ Y^- \longrightarrow Ar\overset{+}{\underset{NO_2}{H}} + Y^- \quad (10)$$

$$Ar\overset{+}{\underset{NO_2}{H}} + Y^- \xrightarrow{\text{fast}} ArNO_2 + HY \quad (11)$$

occur spontaneously with no discrimination among reactive intermediates to accord with the absence of a deuterium kinetic isotope effect. The latter is not consistent with the collapse of the triad in eq 9 initially as an ion pair by proton transfer to the very weakly basic trinitromethide. Furthermore, the presence of extra trinitromethide (deliberately added as the tetrabutylammonium salt) exerts essentially no influence on either the course or the kinetics. Accordingly, the trinitromethide is mainly an innocuous bystander insofar as the disappearance of $ArH^{\bullet+}$ with nitrogen dioxide is concerned; and from the susceptibility of various aromatic cation radicals (prepared by other experimental methods, especially electrochemical oxidation[23]) to nuclear addition,[24] the process in eq 9 can be deduced as that depicted in eqs 10 and 11 (Scheme II). The σ-adduct in eq 10 is the Wheland intermediate in electrophilic nitration,[5] which is known to show no deuterium kinetic isotope effect upon the subsequent deprotonation (eq 11).[25] According to Scheme II, the distribution among the various isomeric Wheland intermediates is established during the collapse of the ion radical pair in eq 10. Consequently, the isomer distributions of the nitration products relate directly to the relative rates of addition of NO_2 to the various nuclear positions of $ArH^{\bullet+}$, provided the addition is irreversible and/or the adduct deprotonates rapidly. Thus the strong correlation between the spin densities at the various nuclear positions of $ArH^{\bullet+}$ and the isomeric product distribution, that was previously noted for aromatic nitration,[26] bears directly on the mechanism of such an ion radical pair collapse to the Wheland intermediate.

(23) See: Yoshida, K. *Electrooxidation in Organic Chemistry*; Wiley: New York, 1984.
(24) Hammerich, O.; Parker, V. D. *Adv. Phys. Org. Chem.* **1984**, *20*, 55.
(25) Melander, L. *Isotope Effects on Reaction Rates*; Ronald: New York, 1960.
(26) Pederson, E. B.; Petersen, T. E.; Torsell, K.; Lawesson, S. O. *Tetrahedron* **1973**, *29*, 579. See also: Fukuzumi, S.; Kochi, J. K. *J. Am. Chem. Soc.* **1981**, *103*, 7240. Lau, W.; Kochi, J. K. *J. Am. Chem. Soc.* **1986**, *108*, 6720.

Although the Wheland intermediate in Scheme II has not yet been separately observed, the time-resolved spectral changes of the cation radical $ArH^{\bullet+}$ do provide insight as to how it is formed. For example, the well-resolved absorption spectrum of the transient aromatic cation radical in Figure 4a that is spontaneously generated by the charge-transfer excitation of the TNM complex is followed by the first-order decay of the ($ArH^{\bullet+}$) absorbance back to the base line (Figure 4b). Since only charge-transfer nitration occurs under these conditions, the experimental first-order rate constant relates solely to the collapse of the ion radical pair to the Wheland intermediate, i.e.,

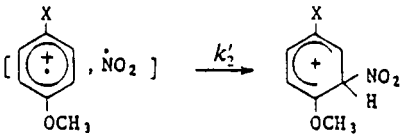

(12)

Indeed the regiospecificity of such an ion radical pair collapse yields the isomeric mixture of nuclear nitration products that is essentially indistinguishable from that obtained under conventional electrophilic conditions.[17,22] It is also worth noting that the byproducts from these CT nitrations are the same as those previously reported in the electrophilic nitration with nitric acid.[7] In particular, the demethylation of the methoxy group to afford nitrophenols and the trans-bromination of 4-bromoanisole to afford a mixture of 4-nitroanisole and 2,4-dibromoanisole are both symptomatic of radical-pair collapse at the ipso positions. These produce the σ-adducts which are akin to the Wheland intermediates known to undergo such transformations.[27]

The kinetics of the collapse of the ion radical pair $[ArH^{\bullet+},NO_2]$ from representative arenes are summarized in Table I, in which the decay of the spectral transients for nitration in eq 10 is a reflection of the stability of the aromatic cation radical. For example, the cation radical from *p*-methylanisole decays by second-order kinetics similar to the kinetic behavior of the long-lived cation radical from *p*-methoxyanisole.[22] The large difference in the rates of diffusive combination with NO_2 in Table I (see column 4) corresponds to their relative stabilities as measured by ΔE° = 8.5 kcal mol^{-1} of the parent arenes (column 1). There is a fur-

(27) For a discussion, see: Kochi, J. K. *Acta Chem. Scand.* **1990**, *44*, 409.

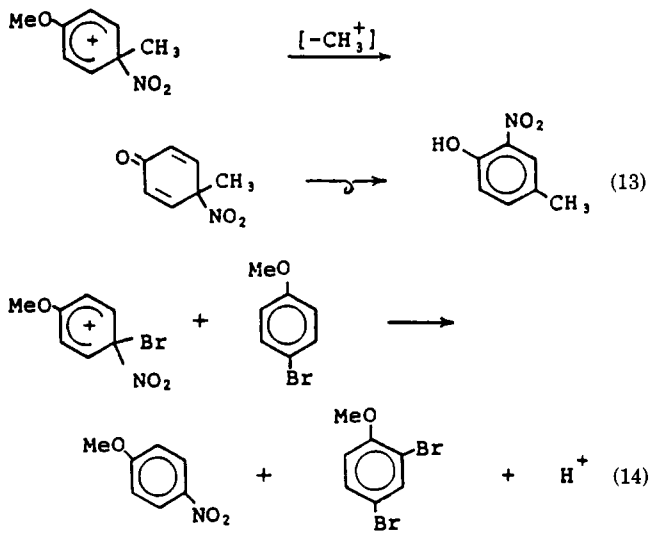

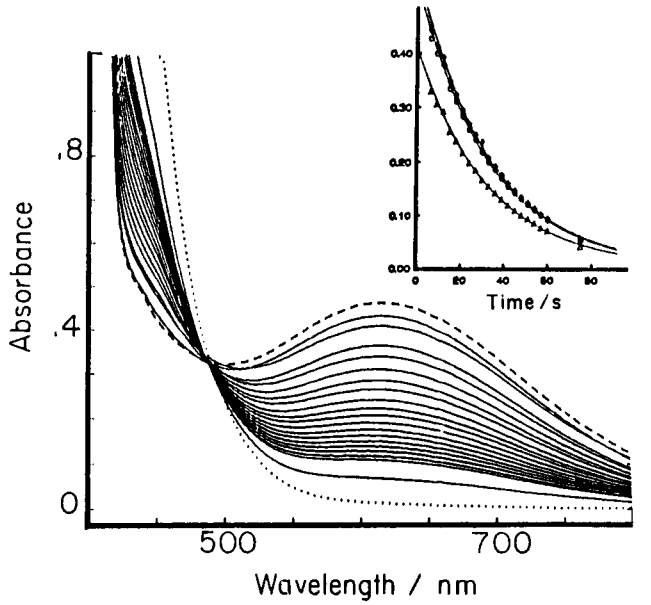

Figure 5. Absorbance change immediately following (---) the addition of $PyNO_2^+$ to an aromatic donor (9-methylanthracene) in acetonitrile and at regular intervals until completion at 5 min (···). The smooth curves in the inset show calculated fit of absorbance change at 600 (◆), 700 (△), and 650 (○) nm to first-order kinetics.[15]

ther, larger gap of $\Delta E° = 10.4$ kcal mol^{-1} which separates the stabilities of the cation radicals of *p*-methylanisole and *p*-fluoroanisole, the least reactive haloanisole. Strikingly, every member of the family of *p*-haloanisole cation radicals reacts with NO_2 by first-order kinetics. This decay pattern strongly suggests that the CT nitration occurs by the cage collapse of the geminate radical pair $[ArH^{\bullet+},NO_2]$ prior to diffusive separation, except when the anisole cation is a relatively stabilized species such as those with *p*-methyl and *p*-methoxy substituents.

Relevance of Charge-Transfer Complexes to Electrophilic (Adiabatic) Nitration

The spectral changes that accompany electrophilic aromatic nitration are shown in Figure 5 by (a) the immediate appearance of the charge-transfer band at $\lambda_{CT} = 612$ nm upon mixing the nitrating agent $X\text{-}PyNO_2^+$ with excess arene $[ArH]_0$ in the dark, followed by (b) the first-order decay (k_{obs}) of the CT absorbance (A_{CT}) back to the base line given as[15]

$$-dA_{CT}/A_{CT} = k_2K_{EDA}[ArH]_0(K_{EDA}[ArH]_0 + 1)^{-1}\,dt \quad (15)$$

The second-order rate constant k_2 and the formation constant K_{EDA} are evaluated from the dependence of k_{obs}^{-1} as a function of the arene concentration $[ArH]_0^{-1}$.

Scheme III

$$[ArH, NO_2^+] \longrightarrow [ArH^{+\cdot}, NO_2^{\cdot}] \quad (16)$$

$$[ArH^{+\cdot}, NO_2] \xrightarrow{k_c} Ar(H)NO_2 \quad (17)$$

$$[ArH^{+\cdot}, NO_2] \xrightarrow{k_d} ArH^{+\cdot} + NO_2\text{, etc.} \quad (18)$$

Table I.
Kinetics of Ion Radical Pair Collapse during Charge-Transfer Nitration[a]

$E°_{ArH}$, V vs SCE	4-XC_6H_4OMe: X	kinetics order	rate constant[b]
1.30	methoxy	2°	1.0×10^4
1.67	methyl	2°	2.5×10^5
1.78	bromo	1°	3.7×10^4
2.00	chloro	1°	2.4×10^4
2.12	fluoro	1°	1.9×10^4

[a] From ref 22. [b] Units of A^{-1} s^{-1} for second-order and s^{-1} for first-order kinetics.

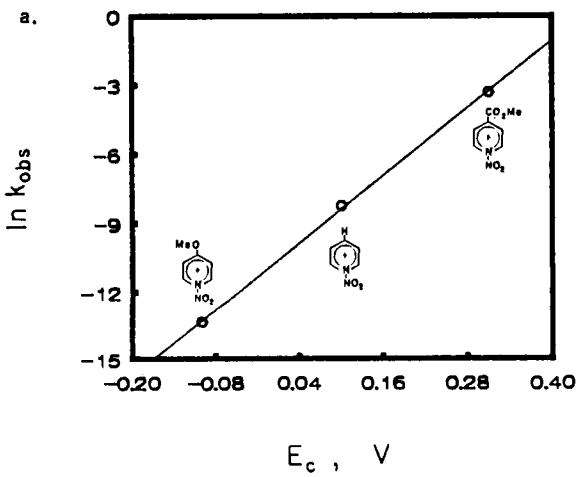

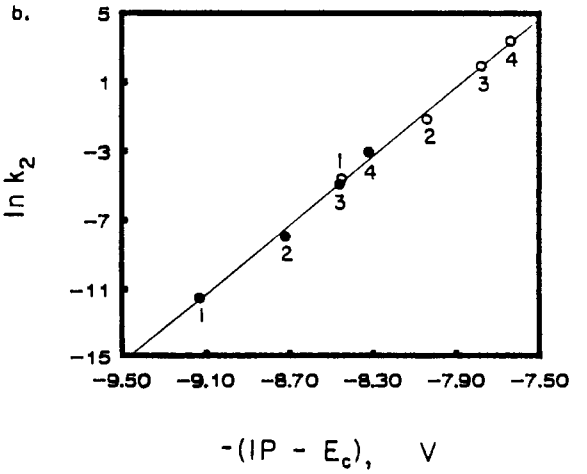

Figure 6. Rate dependence of electrophilic substitution with (a) the acceptor strengths of $X\text{-}PyNO_2^+$ as measured by k_{obs} for 9-methylanthracene and (b) the (HOMO–LUMO) gap of $[ArH,X\text{-}PyNO_2^+]$ complexes with X = H (●) and MeO_2C (○) and ArH = benzene (1), toluene (2), *m*-xylene (3), and mesitylene (4) as measured by k_2 calculated from the competition method in ref 15.

Table II.
Reversible Reduction Potentials and Heterogeneous Electron Transfer Rate Constants for Nitronium and Nitrosonium Cations[a]

solvent	Z^b	DN[c]	$E°$, V[d]		k_s, cm s^{-1}	
			NO_2^+	NO^+	NO_2^+	NO
CH_2Cl_2	64.7	0.0	1.03	1.00	0.017	0.008
CH_3NO_2	71.2	2.7	0.98	0.98	0.015	0.005
CH_3CN	71.3	14.1	0.91	0.87	0.032	0.005
sulfolane	77.5	14.8	0.76	0.76	0.01	0.001
EtOAc	59.4	17.1	0.71	0.75	0.019	0.003
DMF	68.4	26.6		0.56		0.006

[a] From ref 32b. [b] Kosower Z value and [c] Gutmann donor number in kcal mol^{-1} from ref 33. [d] Versus Cp_2Fe.

The linear correlation of the rate of electrophilic nitration with the acceptor strength of X–$PyNO_2^+$ is shown in Figure 6a. The corresponding relationship of the nitration rate with the HOMO–LUMO gap in the [ArH,X–$PyNO_2^+$] complex,[11] as shown in Figure 6b, relates directly to the CT energy of the ion radical pair (compare eq 4). The latter coupled with the common complexion of the nitration products and byproducts underscores the strong similarity between electrophilic aromatic nitration and the mechanism of charge-transfer nitration established by time-resolved spectroscopy. As such, the most *economical* formulation for electrophilic nitration would also include a pathway which is common to charge-transfer nitration, namely, via the ion radical pair I, as presented in eq 2. At one extreme of a very short lifetime, the ion radical pair I is tantamount to the transition state for the concerted one-step process.[28] At the other extreme of a very long lifetime, the ion radical pair is manifested by its diffusive separation. Scheme III presents this simple construct in a kinetics context.[5] The extent to which $k_d \gg k_c$ allows side reactions to compete as a result of the diffusive separation,[29] and it is especially applicable to stable aromatic cation radicals which undergo the subsequent diffusive recombination of $ArH^{\bullet+}$ and NO_2 by second-order kinetics with high efficiency. According to Scheme III, the byproducts can arise via the intermolecular trapping of $ArH^{\bullet+}$ to afford biaryls,[17] and the spontaneous fragmentation of labile $ArH^{\bullet+}$ derived from such aromatic donors as dianthracene, benzpinacols, etc., in the course of electrophilic nitration.[15] The efficient collapse of the ion radical pair to the Wheland intermediate is represented by $k_c \gg k_d$. Such a direct collapse of the ion radical pair has it counterpart in CT nitration by the observed first-order decay of the spectral transients (compare eq 12). However, the observed rate constants in Table I are at least 5 orders of magnitude slower than that expected from the diffusional correlation times of 10^{-10}–10^{-11} s. In other words, if these rate constants relate to the cage collapse of the ion radical pair, then how can I avoid diffusive separation prior to the formation of the Wheland intermediate? In order to address this important point, it is necessary to examine *directly* the association of the pertinent pair of redox couples, viz.,[30]

$$ArH + NO_2^+ \rightleftharpoons ArH^{\bullet+} + NO_2 \qquad (19)$$

For this kinetics study, the closely related cationic electrophile nitrosonium (NO^+) is employed, since various aromatic combinations with nitronium salts such as $NO_2^+BF_4^-$, $NO_2^+SbCl_6^-$, etc. cannot be manipulated, owing to the encounter-controlled nitration.[31] Before doing so, however, the quantitative comparison of the redox behavior of NO_2^+ and NO^+ is required.

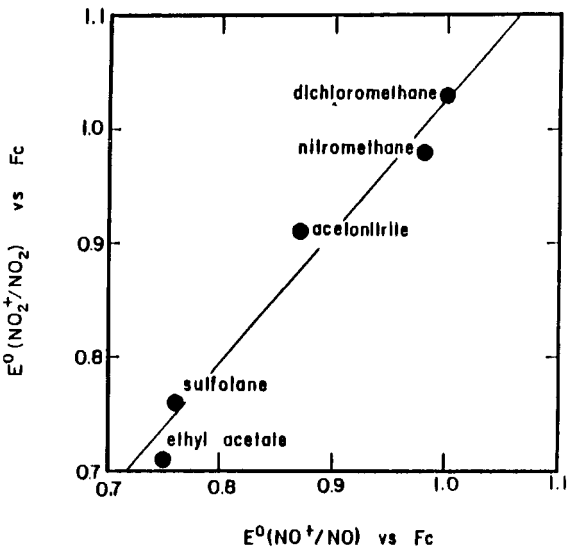

Figure 7. Correlation of the reduction potentials of NO_2^+ and NO^+ in various solvents. The line is arbitrarily drawn with a slope of unity to identify their close similarity. Reprinted with permission from ref 32a. Copyright 1991 American Chemical Society.

Electron-Transfer Equilibria and Kinetics for Nitronium and Nitrosonium Acceptors

The reversible reduction potentials ($E°$) of NO_2^+ and NO^+ as well as the electron-transfer rate constants (k_s) at platinum are established by transient electrochemical techniques in the various solvents listed in Table II.[32] With both cations, $E°$ varies monotonically as a function of the solvent donor number,[33] and this leads to the linear correlation in Figure 7 with a slope of unity. Such a striking similarity in the redox behavior of NO_2^+ and NO^+ is understandable if cognizance is taken of their mutually small size and coordinative unsaturation. Moreover, this strong parallel extends to the kinetics barrier to electron transfer in solution, as measured by the heterogeneous rate constant $k_s = A \exp[-(\Delta G^* + w)/RT]$, where w is the electrostatic work term required

(28) Compare: Pross, A. *J. Am. Chem. Soc.* **1986**, *108*, 3537. Parker, V. D.; Tilset, M. *J. Am. Chem. Soc.* **1987**, *109*, 2521.
(29) Johnston, J. F.; Ridd, J. H.; Sandell, J. P. B. *J. Chem. Soc., Chem. Commun.* **1989**, 244.
(30) Morkovnik, A. S. *Russ. Chem. Rev.* **1988**, *57*, 144. Boughriet, A.; Wartel, M. *J. Chem. Soc., Chem. Commun.* **1989**, 809.
(31) Hoggett, J. G.; Moodie, R. B.; Schofield, K. *J. Chem. Soc. B* **1969**, 1. Olah, G. A. *Acc. Chem. Res.* **1971**, *4*, 241. Ridd, J. H. *Acc. Chem. Res.* **1971**, *4*, 248. See also: Rys, P. *Angew. Chem., Int. Ed. Engl.* **1977**, *16*, 807.
(32) (a) Lee, K. Y.; Amatore, C.; Kochi, J. K. *J. Phys. Chem.* **1991**, *95*, 1285. (b) Lee, K. Y.; Kuchynka, D. J.; Kochi, J. K. *Inorg. Chem.* **1989**, *28*, 567.
(33) Reichardt, C. *Solvent and Solvent Effects in Organic Chemistry*, 2nd ed.; VCH: New York, 1989.

to transport the electroactive species from the bulk solution to the electrode. According to the preequilibrium model,[34] the preexponential factor $A = 3 \times 10^5$ cm s^{-1} and it drops out in the comparison of the relative rates, i.e.,

$$k_{s1}/k_{s2} = \exp[-(\Delta G^{\ddagger}_1 - \Delta G^{\ddagger}_2 + w_1 - w_2)/RT] \quad (20)$$

where the subscripts 1 and 2 refer to the NO_2^+/NO_2 and NO^+/NO couples, respectively. The work term describes the average electrostatic interaction, and it is (according to the Gouy–Chapman–Stern model of the diffuse double layer) directly related to the charge density on the electrode and most importantly determined by the potential.[35] Since NO_2^+ and NO^+ are reduced in the same potential range (and they are of roughly comparable size), the difference in work terms is likely to be small. Accordingly, the difference in activation free energy for electron transfer can be approximated as

$$\Delta G^{\ddagger}_1 - \Delta G^{\ddagger}_2 \simeq -RT \ln k_{s2}/k_{s1} \quad (21)$$

From the measured values of k_s for NO_2^+ and NO^+ in Table II, the free energy difference is evaluated as only 1.1 kcal mol^{-1}. Thus the slower rate of heterogeneous electron transfer to NO^+ results from a reorganization energy which is actually ~4 kcal mol^{-1} *higher* than that for NO_2^+. In outer-sphere electron transfer, such an energy difference arises from the reorganization energies that can be calculated from the stretching and bending force constants and the structural parameters of the nitrogen oxides.[36] However, the reorganization energy $\lambda_i = 78$ kcal mol^{-1} for NO_2^+ is calculated to be substantially greater than $\lambda_i = 21$ kcal mol^{-1} for NO^+ when electron transfer proceeds via an outer-sphere activated complex.[37] The failure of Marcus theory to account for the significantly faster rate for the electrochemical reduction of NO_2^+ relative to NO^+ is attributed to the participation of an inner-sphere pathway.[38] Indeed the strong dependence of $E°$ on solvent donicity (see Table II) underscores the importance of NO_2^+ and NO^+ coordination as an indication of the inner-sphere activated complex at the platinum electrode.[39] Importantly, the thermodynamic and kinetic similarity of NO_2^+ and NO^+ at platinum encourage the use of the analogous aromatic redox couple,[30]

$$ArH + NO^+ \rightleftharpoons ArH^{\bullet+} + NO \quad (22)$$

as an appropriate solution model for the electron-transfer dynamics pertinent to aromatic nitration (eq 19) in the following manner.

Outer-Sphere and Inner-Sphere Mechanisms for Electron Transfer of Nitrosonium

The 1:1 EDA complexes of aromatic donors with nitrosonium are characterized by (visible) charge-transfer bands[40] similar to those presented in Figure 1. The molecular structure of $[ArH,NO^+PF_6^-]$ established by X-ray crystallography[41] is presented in the ORTEP diagram below as the oblique (bent) orientation of the nitrosonium acceptor poised centrally over the mesitylene ring.[42]

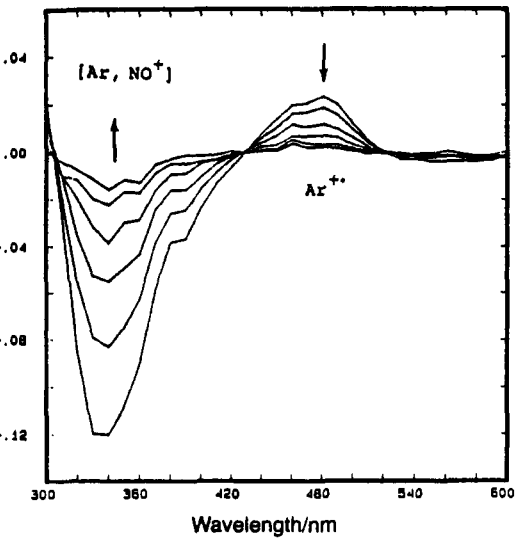

Figure 8. Typical time-resolved absorption spectrum following the CT excitation of nitrosonium EDA complexes with arene (hexamethylbenzene) showing the bleaching of the CT absorption band and the concomitant growth of the aromatic cation radical ($HMB^{\bullet+}$).[44]

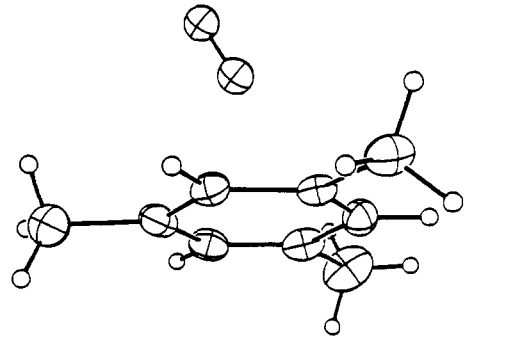

Since the closest approach of NO^+ to an aromatic carbon of 2.5 Å exceeds the distance for conventional bonding, the nonbonded EDA complex is held together solely by charge-transfer interactions of the type described for the various nitrating acceptors NO_2Y (vide supra).[43]

The charge-transfer excitation of the aromatic complexes with NO^+ is initially carried out at $\lambda = 352$ nm using a 30-ns laser pulse. The time-resolved (difference) spectrum in Figure 8 illustrates the typical bleaching of the CT absorption band by the pronounced negative absorption ($\Delta A < 0$), which is accompanied by the concomitant appearance of $ArH^{\bullet+}$,[27] in accord with the expectations of Mulliken theory,[12] i.e.,

$$[ArH,NO^+] \xrightarrow{h\nu_{CT}} [ArH^{\bullet+},NO] \quad (23)$$
$$\text{II}$$

(34) Brunschwig, B. S.; Logan, J.; Newton, M. D.; Sutin, N. *J. Am. Chem. Soc.* **1980**, *102*, 5798. Marcus, R. A. *Int. J. Chem. Kinet.* **1981**, *13*, 865.
(35) Stern, O. *Z. Elektrochem.* **1924**, *30*, 508.
(36) Marcus, R. A. *J. Phys. Chem.* **1963**, *67*, 853; *J. Chem. Phys.* **1956**, *24*, 966; *Annu. Rev. Phys. Chem.* **1964**, *15*, 155.
(37) Eberson, L.; Radner, F. *Acta Chem. Scand.* **1984**, *38B*, 861; *Acc. Chem. Res.* **1987**, *20*, 53. See also: Lee et al., ref 32a.
(38) See: Fukuzumi, S.; Wong, C. L.; Kochi, J. K. *J. Am. Chem. Soc.* **1980**, *102*, 2928.
(39) Compare: Weaver, M. J.; Anson, F. C. *J. Am. Chem. Soc.* **1975**, *97*, 4403; *Inorg. Chem.* **1976**, *15*, 1871.
(40) Reents, W. D., Jr.; Freiser, B. S. *J. Am. Chem. Soc.* **1980**, *102*, 271. Brownstein, S.; Gabe, E.; Lee, F.; Tan, L. *J. Chem. Soc., Chem. Commun.* **1984**, 1566.
(41) Brownstein, S.; Gabe, E.; Lee, F.; Piotrowski, A. *Can. J. Chem.* **1986**, *64*, 1661.
(42) Kim, E. K.; Kochi, J. K. *J. Am. Chem. Soc.* **1991**, *113*, 4962.
(43) Prout, C. K.; Kamenar, B. In *Molecular Complexes*; Foster, R., Ed.; Elek: London, 1973; p 151 ff.

Table III.
Rate and Equilibrium Constants for Outer-Sphere and Inner-Sphere Electron Transfer According to Scheme IV[a]

aromatic donor	K_{EDA}, M^{-1}	$-\Delta G_{OS}$, kcal/mol^{-1}	K_{OS}	k_2, M^{-1} s^{-1}	k_{-2}, M^{-1} s^{-1}
hexamethylbenzene	3.1×10^4	7.8	5.6×10^5	1.9×10^6	4.0
pentamethylbenzene	5.0×10^3	10.4	4.1×10^7	1.0×10^7	0.24
durene	4.5×10^2	11.8	4.2×10^8	2.4×10^7	0.057
p-xylene	30	17.1	3.3×10^{12}	4.1×10^8	1.2×10^{-4}
toluene	5	25.8	8.8×10^{18}	1.2×10^{10}	1.4×10^{-9}

aromatic donor	K_A, M^{-1}	$-\Delta G_{IS}$, kcal mol^{-1}	K_{IS}	k_1, s^{-1}	k_{-1}, s^{-1}
hexamethylbenzene	30	12.0	6.3×10^8	1×10^8	0.16
pentamethylbenzene	11	14.1	2.1×10^{10}	4×10^8	0.20
durene	5	14.5	4.5×10^{10}	7×10^8	0.015
p-xylene	2.3	18.7	5.0×10^{13}	1×10^9	2.8×10^{-5}
toluene	2.2	26.3	1.9×10^{19}	2×10^{10}	1.0×10^{-9}

[a] From ref 44.

Scheme IV

$$\text{II} = [ArH^{+\cdot}, NO] \underset{k_a}{\overset{k_d}{\rightleftharpoons}} ArH^{+\cdot} + NO$$

$$k_{-1} \Big\| k_1 \qquad k_{-2} \Big\| k_2$$

$$[ArH, NO^+] \overset{K_{EDA}}{\rightleftharpoons} ArH + NO^+$$

The subsequent disappearance of $ArH^{\cdot+}$ is shown in the nanosecond-laser studies by the return of the difference absorbances ($\Delta A > 0$) back to the base line within a few microseconds to agree generally with the rate data for nitration in Table I.[27] However, the more detailed picosecond studies reveal the initially formed II in eq 23 to undergo first-order relaxation by back electron transfer (k_1) in competition with diffusive separation (k_d).[44] Coupled with the second-order kinetics observed for longer times in the nanosecond studies, i.e.,

$$ArH^{\cdot+} + NO \rightarrow [ArH,NO^+] \qquad (24)$$

the complete dynamics for the return of the pair of radicals in eq 24 can be summarized as[44] depicted in Scheme IV, and the pertinent rate and equilibrium constants are collected in Table III. The time-resolved spectroscopic studies in Scheme IV thus identify two electron-transfer processes for the return of the aromatic cation radical and nitric oxide, namely, that proceeding directly from the geminate pair [$Ar^{\cdot+}$,NO] and that arising via the freely diffusing species $Ar^{\cdot+}$ and NO, and these are associated with the observed first-order and second-order kinetics. In order to emphasize this kinetics dichotomy, the ground-state preequilibrium (K_{EDA}) for the formation of the EDA complex is included in Scheme IV to complete the thermochemical cycle.

Outer-sphere electron transfer as indicated by the rate constant k_2 in Scheme IV relates to the outer-sphere redox equilibrium with $K_{OS} = k_2/k_{-2}$. As such, the dependence of the electron-transfer rate on the aromatic donor is predicted by the Marcus relationship:[36] $k_2 = Z \exp[-\lambda[1 + \Delta G_{OS}/\lambda]^2/4RT]$, where the reorganization energy is taken as $\lambda = 40$ kcal mol^{-1} [37] and the driving force $-\Delta G_{OS}$ is given by $RT \ln K_{OS} = \mathcal{F}(E^\circ_{ArH} + E^\circ_{NO^+})$. The values of $-\Delta G_{OS}$ and K_{OS} in Table III are based on independent measurements of the reversible oxidation and reduction potentials of the aromatic donor E°_{ArH} and nitrosonium $E^\circ_{NO^+}$, respectively, and the Faraday constant $\mathcal{F}$.[14,32] It is singularly noteworthy that the trend in the experimental values of the second-order rate constant bears no relationship to that of the outer-sphere electron transfer rates predicted by Marcus theory. Clearly, an alternative mechanism must be considered for the return of $ArH^{\cdot+}$ and NO to the original EDA complex.

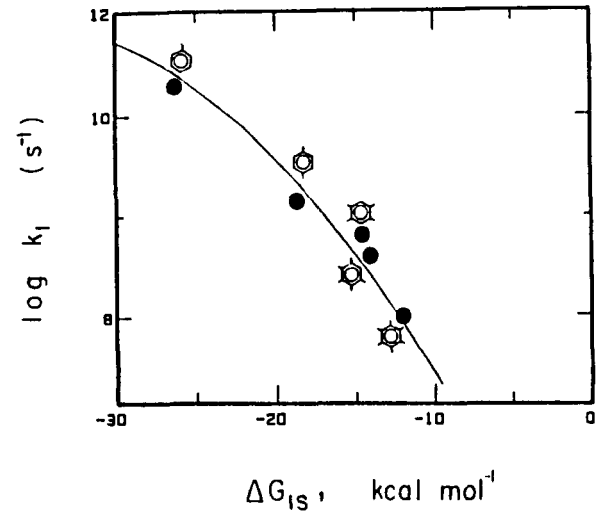

Figure 9. Dependence of the experimental first-order constant k_1 on the inner-sphere driving force ΔG_{IS} for geminate recombination of the cation radical pair [$Ar^{\cdot+}$,NO] in acetonitrile. The smooth curve is calculated from the Marcus equation with $\lambda' = 37$ kcal mol^{-1}.[44]

The *inner-sphere* electron transfer is a more circuitous pathway in Scheme IV since it proceeds via the cation radical pair [$ArH^{\cdot+}$,NO] to the charge-transfer complex [ArH,NO^+] that represents the inner-sphere redox equilibrium with $K_{IS} = k_1/k_{-1}$. The overall second-order rate constant for such an inner-sphere pathway for electron transfer can be described in terms of the preequilibrium association (k_a) and separation (k_d) steps as $k_{II} = k_1 k_a/(k_1 + k_d)$. Most notably, the calculated values of k_{II} based on this steady-state expression agree with the experimental rate constants.[44] If we consider for the moment the inner-sphere electron transfer with a rate-limiting k_1 in the context of the Marcus equation,[36] the driving force $-\Delta G_{IS}$ taken from the thermochemical cycle in Scheme IV is represented as a combination of the outer-sphere contribution ΔG_{OS} and the complexation, i.e., $\Delta G_{IS} = \Delta G_{OS} + \Delta G_{EDA} - \Delta G_A$. The resulting free energy relationship of the electron-transfer rate (log k_1) with the driving force ($-\Delta G_{IS}$) is shown by the smooth curve in Figure 9. Since the optimized reorganization energy of $\lambda' = 37$

(44) Bockman, T. M.; Karpinski, Z. J.; Sankararaman, S.; Kochi, J. K. *J. Am. Chem. Soc.*, in press.

kcal mol^{-1} is close to the corresponding outer-sphere barrier (vide supra), it suggests that the transition states for the k_1 and k_2 processes bear a strong resemblance to each other.[45] In other words, the mechanistic distinction between the inner-sphere and outer-sphere electron transfer of $ArH^{\bullet+}$ and NO lies in the formation (K_A) of the (inner-sphere) cation radical pair [$ArH^{\bullet+}$, NO] as the *kinetically dominant intermediate.*

Conclusions

Comparative product studies and time-resolved spectroscopy following the charge-transfer excitation of aromatic complexes with NO_2Y demonstrate the ion radical pair [$ArH^{\bullet+}$,NO_2] to be a viable intermediate in aromatic nitration, in accord with Olah's thesis of a second reactive intermediate.[3,15] Electron transfer in eq 2 occurs via the inner-sphere mechanism, as judged by the microdynamical behavior of the closely related ion radical pair [$ArH^{\bullet+}$,NO] in Scheme IV.[46] As such, other attempts[30] to quantitatively evaluate the electron-transfer mechanism by the indiscriminate application of Marcus theory for *outer-sphere* electron transfer are conceptually flawed.[47]

I thank my colleagues, especially S. Sankararaman, E. K. Kim, T. M. Bockman, and K. Y. Lee, for their tireless efforts to fathom the intricacies of electron-transfer dynamics and mechanisms of the nitrogen oxides, and the National Science Foundation, Robert A. Welch Foundation, and Texas Advanced Research Program for financial support.

(45) Hammond, G. S. *J. Am. Chem. Soc.* **1955**, *77*, 334.

(46) For the inner-sphere structures of such nonbonded donor–acceptor complexes, see ref 42. Analogously, the inner-sphere character of the ion radical pair in nitration is likely to be reflected in a bent NO_2 moiety in the nonbonded structure of I. Further studies are in progress to reconcile the first-order kinetics in Table I and Figure 4b.

(47) For an early caveat, see the following: Fukuzumi, S., et al., ref 38. Kochi, J. K. *Angew. Chem., Int. Ed. Engl.* **1988**, *27*, 1227.

Three-Center, Two-Electron C–H–C Bonds in Organic Chemistry†

JOHN E. MCMURRY* and THOMAS LECTKA

Department of Chemistry, Baker Laboratory, Cornell University, Ithaca, New York 14853

Received October 10, 1991 (Revised Manuscript Received November 6, 1991)

To organic chemists, covalent bonding is synonymous with the sharing of two electrons between two atomic centers. The stable substances we usually work with contain only such two-center, two-electron bonds: C–H, C–C, C–O, and so forth. Inorganic and organometallic chemists, however, are used to dealing with a much richer diversity of bonding patterns that often includes the sharing of two electrons between *three* atomic centers. Such three-center, two-electron bonds (3c–2e) are particularly common in the boron hydrides, but are also found in bridged metal halides, bridged metal alkyls, metal–hydrogen agostic interactions, and many other systems.

Three-center, two-electron bonding is not, of course, limited to inorganic and organometallic chemistry. Such bonding also occurs in organic chemistry, but the instances of its occurrence are relatively few, and the substances that contain these bonds are relatively unstable.[1] Several kinds of 3c–2e bonds are possible in organic chemistry, and it is useful to distinguish between the "open" or "unsupported" situation and the "closed" or "supported" one.[2] Open 3c–2e bonds are those wherein the geometry is roughly linear so that there is negligible bonding interaction between the terminal atoms. Closed 3c–2e bonds are those wherein the geometry is acutely triangular so that there is a bonding interaction among all three atoms. Of course, the two situations are merely the extremes of a bonding continuum. Note that organic substances showing 3c–2e bonding must be cations and that one or more of the atoms involved—either carbon or hydrogen—must be "hypervalent". That is, one or more of the carbon atoms must be pentavalent or one or more of the hydrogens must be divalent.

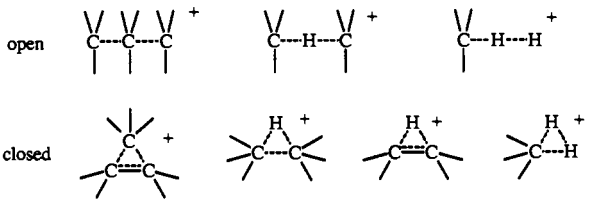

A molecular orbital description of 3c–2e bonding shows a doubly occupied bonding MO, along with

John E. McMurry, Professor of Chemistry at Cornell University and Associate Editor of *Accounts of Chemical Research* since 1975, has provided biographical scraps in several previous Accounts. His scientific interests include the development of synthetic-organic methodology, the total synthesis of unusual molecules, and the writing of undergraduate texts.

Thomas Lectka, a native of Detroit, MI, received his B.A. from Oberlin College in 1985 and his Ph.D. from Cornell University in 1991. Following his doctoral work, the subject of which forms the basis of this Account, he spent a year as an Alexander von Humboldt Fellow in the laboratory of Professor Rolf Gleiter at Heidelberg and then moved to Harvard University for further postdoctoral work with David Evans. His research interests include a blend of synthetic organic, physical organic, and computational problems.

†It is a great pleasure to dedicate this paper to my friend and colleague Professor Joseph Bunnett, whose vision and hard work made this journal the outstanding success that it is today.

(1) For reviews of three-center, two-electron bonds in organic chemistry, see: (a) Olah, G. A.; Surya Prakash, G. K.; Williams, R. E.; Field, L. D.; Wade, K. *Hypercarbon Chemistry*; Wiley-Interscience: New York, 1987. (b) DeKock, R. L.; Bosma, W. B. *J. Chem. Educ.* **1988**, *65*, 194–197.

(2) Bau, R.; Teller, R. G.; Kirtley, S. W.; Koetzle, T. F. *Acc. Chem. Res.* **1979**, *12*, 176–183.

0001-4842/92/0125-0047$03.00/0